Rome Preprint 1157/96
SNS/PH/1996-007
SWAT/133
FTUV 96/73 - IFIC 96/82

Light Quenched Hadron Spectrum and Decay Constants on different Lattices

C.R. Allton

Department of Physics, University of Wales Swansea, Singleton Park, Swansea SA2 8PP, United Kingdom

V. Giménez

Dep. de Fisica Teorica and IFIC, Univ. de València, Dr. Moliner 50, E-46100, Burjassot, València, Spain

L. Giusti

Scuola Normale Superiore, P.za dei Cavalieri 7 - I-56100 Pisa Italy
INFN Sezione di Pisa I-56100 Pisa Italy

F. Rapuano

Dipartimento di Fisica, Università di Roma 'La Sapienza' and INFN, Sezione di Roma, P.le A. Moro 2, I-00185 Roma, Italy.

Abstract

In this paper we study $\mathcal{O}(2000)$ (quenched) lattice configurations from the APE collaboration, for different lattice volumes and for $6.0 \leq \beta \leq 6.4$ using both the Wilson and the SW-Clover fermion actions. We determine the light hadronic spectrum and meson decay constants and study the mesonic dispersion relation. We extract the hadronic variable J and the strange quark mass in the continuum at the next-to-leading order obtaining $m_s^{\overline{MS}}(\mu = 2GeV) = 122 \pm 20\ MeV$. A study is made of their dependence on lattice spacing. We implement a newly developed technique to extract the inverse lattice spacing using data at the *simulated values* of the quark mass (i.e. at masses around the strange quark mass).

PACS: 11.15.H, 12.38.Gc, 13.30.Eg, 14.20.-c and 14.40.-n

1 Introduction

The lattice technique has proved a very effective theoretical tool to determine phenomenological quantities such as the mass spectrum and weak decay matrix elements. Unlike other approaches, it does not (in principle) suffer from uncontrolled approximations. However, in practice, one is forced to work on a lattice of (i) finite size, with (ii) a finite lattice spacing, and (iii) unphysically large masses for the light quarks. Also the quenched approximation is often used in lattice studies. In this work we determine the light hadronic spectrum and meson decay constants and we study the effects of (i), (ii) and (iii), and in particular, we try to overcome some of the inherent approximations corresponding to (iii). It is important to study the systematics due to (i), (ii) and (iii) before the effects of the quenched approximation can be correctly understood.
The results reported in this paper are obtained from $\mathcal{O}(2000)$ (quenched) lattice configurations from the APE collaboration, for different lattice volumes and for $6.0 \leq \beta \leq 6.4$ using both the Wilson action and the SW-Clover fermion action. In this range of β we cannot draw any conclusion about a dependence of hadron masses and pseudoscalar decay constants. On the other hand we find that the quenched approximation gives a resonable agreement with the experimental values.
The plan of the paper is as follows. In the next section details of the simulations are given. Sect. 3 describes the method used to determine the spectrum and matrix elements from the lattice data. The results on hadron masses, meson decay constants, J values, meson dispersion relations and quark masses are then presented in Sect. 4, with a comparison with results from other collaborations. In the last section we report our concluding remarks.

2 Lattice Details

In the last four years the APE group has been extensively studying lattice QCD in the quenched approximation. The lattice data used in this study come from $\mathcal{O}(2000)$ configurations generated by the APE collaboration primarily to study weak matrix elements such as f_D, f_B and B_K and semileptonic decays [1]-[7]. The data have been obtained from eight sets of configurations with $\beta = 6.0$, 6.2 and 6.4. The quark propagators have been obtained from either the Wilson action or the 'improved' SW-Clover action, by the standard APE inversion procedure[8]. The hopping parameters and the other parameters used in each simulation are listed in Table 1. These K values correspond to quark masses roughly in the range of the strange quark mass which are adequate for the primary goal of the runs described before. In the past the APE collaboration has introduced the so called 'smearing' technique [8] in or-

Table 1
Summary of the parameters of the runs analyzed in this work. T-Sweeps stands for thermalising Montecarlo sweeps performed starting from a cold configuration and I-Sweeps stands for the number of sweeps after which independent configurations are gathered.

	C60	W60	C62a	W62a	C62b	W62b	W64	C64
Ref	[1]-[3]	[1,4]	[6]	[6]	[7]	[4,5]	[6]	[6]
β	6.0	6.0	6.2	6.2	6.2	6.2	6.4	6.4
Action	SW	Wil	SW	Wil	SW	Wil	Wil	SW
# Confs	200	320	250	250	200	110	400	400
Volume	$18^3 \times 64$	$18^3 \times 64$	$24^3 \times 64$	$24^3 \times 64$	$18^3 \times 64$	$24^3 \times 64$	$24^3 \times 64$	$24^3 \times 64$
T-Sweeps	3000	3000	5000	5000	3000	3000	7000	7000
I-Sweeps	800	800	2000	2000	800	2400	3000	3000
K	-	-	0.14144	0.1510	-	-	0.1488	0.1400
	0.1425	0.1530	0.14184	0.1515	0.14144	0.1510	0.1492	0.1403
	0.1432	0.1540	0.14224	0.1520	0.14190	0.1520	0.1496	0.1406
	0.1440	0.1550	0.14264	0.1526	0.14244	0.1526	0.1500	0.1409

der to have a better determination of the lowest state mass. The APE group has compared data extracted from smeared and non-smeared propagators and found no real improvement on lattices of a time extension of 64 sites at $\beta = 6.0$ and $\beta = 6.2$ [5]. The data presented in this work are obtained without any smearing procedure. In fact the data from W64 and C64 seem to suggest that a smearing procedure would have increased the reliability of the extraction of the mass of the lowest lying states. We plan to increase the time extension of this lattice and check the validity of the 'local' data presented here.
A further comment is due regarding the 'thinning' procedure [8] used to reduce memory occupation. In this technique, correlation functions are computed taking only one point out of three in each space direction. We have checked that this procedure does not affect the physical quantities extracted from the two point correlation functions. All baryonic data presented in this paper come from 'thinned' propagators while mesonic correlation functions come from the full lattice.
Note that the simulations have been performed at β values of 6.0 or larger. This is to negate the large systematic error present in lattice data for $\beta \lesssim 6.0$ due to lattice artifacts. A clear signal for these systematics is the lack of scaling amongst different physical quantities (see, for example, table 2 of [9] and [10]).

Hadron masses and decay constants have been extracted from two-point cor-

relation functions in the standard way. For the meson masses and decay constants we have computed the following propagators:

$$\begin{aligned} G_{55}(t) &= \sum_x \langle P_5(x,t) P_5^\dagger(0,0)\rangle \ , \\ G_{05}(t) &= \sum_x \langle A_0(x,t) P_5^\dagger(0,0)\rangle \ , \end{aligned} \tag{1}$$

where

$$\begin{aligned} P_5(x,t) &= i\bar{q}(x,t)\gamma_5 q(x,t) \ , \\ A_\mu(x,t) &= \bar{q}(x,t)\gamma_\mu\gamma_5 q(x,t) \ . \end{aligned}$$

and the following propagators of the vector states:

$$G_{ii}(t) = \sum_{i=1,3} \sum_x \langle V_i(x,t) V_i^\dagger(0,0)\rangle \ , \tag{2}$$

where

$$V_i(x) = \bar{q}(x,t)\gamma_i q(x,t) \ .$$

In order to determine the baryon masses we have evaluated the following propagators:

$$\begin{aligned} G_n(t) &= \sum_x \langle N(x,t) N^\dagger(0,0)\rangle \ , \\ G_\delta(t) &= \sum_x \langle \Delta_\mu(x,t) \Delta_\mu^\dagger(0,0)\rangle \ , \end{aligned} \tag{3}$$

where

$$\begin{aligned} N &= \epsilon_{abc}(u^a C\gamma_5 d^b) u^c \\ \Delta_\mu &= \epsilon_{abc}(u^a C\gamma_\mu u^b) u^c \ . \end{aligned}$$

For some meson correlation functions, non-zero momentum values were also studied (see section 4.2).
We fit the zero-momentum correlation functions in eqs. 1, 2 and 3 to a single particle propagator with *cosh* or *sinh* in the case of mesonic and axial-pseudoscalar correlation functions and with an *exp* function in the case of the baryonic correlation functions

$$G_{55}(t) = \frac{Z^{55}}{M_{PS}} \exp(-\frac{1}{2} M_{PS} T) \cosh(M_{PS}(\frac{T}{2} - t)) \ ,$$

Table 2
Time interval for baryons and mesons used in the fits for all lattices and for all momenta.

	C60	W60	C62a	W62a	C62b	W62b	W64	C64
Mesons with zero momentum								
	15-28	15-28	18-28	18-28	18-28	18-28	24-30	24-30
Mesons with non-zero momentum								
$p^2 = 1$	10-20	10-20	12-20	12-20	12-20	-	17-27	17-27
$p^2 = 2$	10-20	10-20	11-16	11-16	10-15	-	17-22	17-22
$p^2 = 3$	10-15	10-15	11-16	11-16	-	-	-	-
Baryons with zero momentum								
	12-21	12-21	18-28	18-28	18-28	18-28	22-28	22-28

$$
\begin{aligned}
G_{ii}(t) &= \frac{Z^{ii}}{M_V} \exp(-\frac{1}{2} M_V T) \cosh(M_V(\frac{T}{2} - t)) \ , \\
G_{05}(t) &= \frac{Z^{05}}{M_{PS}} \exp(-\frac{1}{2} M_{PS} T) \sinh(M_{PS}(\frac{T}{2} - t)) \ , \\
G_{n,\delta}(t) &= C^{n,\delta} \exp(-M_{n,\delta} t) \ ,
\end{aligned}
\tag{4}
$$

in the time intervals reported in Table 2. In eqs. 4, T represents the lattice time extension, the subscripts PS and V stand for pseudoscalar and vector meson, n and δ stand for nucleon- and delta-like baryons[1]. To improve stability, the meson (axial-pseudoscalar) correlation functions have been symmetrized (anti-symmetrized) around $t = T/2$. The time fit intervals are chosen with the following criteria: we fix the lower limit of the interval as the one at which there is a stabilization of the effective mass, and, as the upper limit the furthest possible point before the error overwhelms the signal. We discard the possibility of fitting in a restricted region where a plateau is present, as the definition of such a region is questionable [11]. For lattices with highest number of configurations, i.e. W60, W64 and C64, we confirm that a higher statistics does not lead to a longer or better (relative to statistical errors) plateau [11]. The results of these fits for each run are reported in Tables 3-10. Representative examples of the effective mass plots can be seen in Figs. 1 - 4 in the case of W60 for the heaviest $K = 0.1530$. The errors have been estimated by a jacknife procedure, blocking the data in groups of 10 configurations and we have checked that there are no relevant changes in the error estimate by blocking groups of configurations of different size. We have also attempted to

[1] i.e. n stands for the nucleon N, $\Lambda\Sigma$ or Ξ baryon, and δ is either a Δ^{++} or a Ω.

fit the first excited state mass for the mesons with a two hyperbolic cosine fit but the results are rather unstable and noisy on all lattices and will not be reported here. A similar conclusion holds for the baryonic parity partners.

The pseudoscalar and vector decay constants f_{PS} and $1/f_V$ are defined through the equations

$$\langle 0|A_0|PS\rangle = i\frac{f_{PS}}{Z_A}M_{PS} \ , \tag{5}$$

$$\langle 0|V_i|V,r\rangle = \epsilon_i^r \frac{M_V^2}{f_V Z_V} \ , \tag{6}$$

where ϵ_i^r is the vector-meson polarization, M_{PS} and M_V are the pseudoscalar and vector masses and $Z_{V,A}$ are the renormalization constants. We extract f_{PS} from the ratio

$$\begin{aligned} R_{f_{PS}}(t) &= Z_A\frac{G_{05}(t)}{G_{55}(t)} \\ &\longrightarrow Z_A\frac{Z^{05}}{Z^{55}}\tanh(M_{PS}(\frac{T}{2}-t)) \\ &= Z_A\frac{\langle 0|A_0|P\rangle}{\langle 0|P_5|P\rangle}\tanh(M_{PS}(\frac{T}{2}-t)) \\ &= \frac{f_{PS}M_{PS}}{\sqrt{Z^{55}}}\tanh(M_{PS}(\frac{T}{2}-t)) \ , \end{aligned} \tag{7}$$

and the vector-meson decay constant is obtained directly from the parameters of the fit to $G_{ii}(t)$, eqs. 4:

$$\frac{1}{Z_V f_V} = \frac{\sqrt{Z^{ii}}}{M_V^2} \ . \tag{8}$$

The results of these fits for each run are reported in Tables 3 - 10.

3 Extraction of physical quantities

Once the hadronic correlation functions have been fitted, and the lattice masses and matrix elements extracted, the 'conventional method' of determining physical quantities relies on a number of chiral extrapolations. The first extrapolation is in the lattice pseudoscalar mass squared, $(M_{PS}a)^2$, against $1/K$. This sets the critical kappa value K_c corresponding to zero quark mass.

A second chiral extrapolation is performed of $(M_V a)$ to zero quark mass. Using the experimental value of the ρ mass, $M_V(K_c) = 770\ MeV$, the lattice spacing a is determined (assuming a massless pion).

This conventional method relies on an extrapolation from a region where data has been obtained to a region well beyond the reach of direct simulations, assuming that the pseudoscalar mass follows the predictions of PCAC, and that other physical quantities scale linearly in the quark mass [2]. This problem suggests one should extract as much physics as possible from the 'strange' region and to use chiral extrapolations only where absolutely necessary. The method we use to achieve this aim is outlined below.

- We define the following five 'lattice physical planes' for masses and decay constants: $(M_V a, (M_{PS}a)^2)$, $(f_{PS}a/Z_A, (M_{PS}a)^2)$, $(1/(f_V Z_V), (M_{PS}a)^2)$, $(M_n a, (M_{PS}a)^2)$ and $(M_\delta a, (M_{PS}a)^2)$. We plot the lattice data for each K value used in the simulation on these planes . (See Figs. 5 - 9.)
- On the $(M_V a\ , (M_{PS}a)^2)$ plane we impose the physical ratio $C_{sl} = M_{K^*}/M_K$. This corresponds to find the intercept of the curve

$$M_V a = C_{sl}\sqrt{(M_{PS}a)^2}, \tag{9}$$

  with the linear fit of the lattice data (i.e. the right-hand curve in Fig. 5). Lacock and Michael [13] have used this approach to define the quantity J. (See also [14] and [15].) The intercept of this curve and the simulated data defines $M_K a$ and $M_{K^*}a$ but only one of these is an independent prediction.
- We now use the value of $M_K a$ determined above to read off the lattice meson decay constants, $(f_K a/Z_A)$ and $(f_{K^*}Z_V)^{-1}$ from the corresponding f_{PS} and f_V planes. At this stage we have the following 3 independent predictions: $(M_{K^*}a)$, $(f_K a/Z_A)$ and $(f_{K^*}Z_V)^{-1}$. These were all obtained from the quark mass region actually simulated (see Figs 5, 8 and 9), and hence they do not rely on a chiral extrapolation. [3]
- The lattice spacing a, can simply be set by comparing either $(M_{K^*}a)$ or $(f_K a/Z_A)$ with their experimental value. (f_{K^*} cannot be used since it is dimensionless.) Of these two quantities, we choose M_{K^*} to set the scale whenever we need to quote results in physical units. This is because M_{K^*} is determined experimentally more accurately than f_K, and it has no ambiguities associated with a renormalisation constant. However, for completeness, we list in Table 11 the a^{-1} values obtained from all the quantities.

In this analysis for $M_{K^*}a$, $f_K a/Z_A$ and $(f_{K^*}Z_V)^{-1}$ we have assumed that the quadratic $SU(3)-$flavour breaking effects in the meson masses or decay con-

[2] It is unlikely that the problem of 'chiral logs' in the quenched approximation be visible at the values of the simulated quark masses [12].

[3] Depending on the choice of K, a modest linear extrapolation in M_{PS}^2 may be required. The range of this extrapolation is small and so should not cause problems.

stants can be safely neglected in the range of masses explored here. This means that we assume that the masses and decay constants for mesons, with both degenerate, and non-degenerate constituent quarks, lie on the same universal curve. Studies have shown this to be an entirely reasonable hypothesis for quarks around the strange mass [16].

To proceed to obtain other physical quantities, we need the additional input of quark model considerations, and chiral extrapolations. Therefore the determination of these additional quantities suffers from the same criticisms as outlined above for the conventional approach. Consider the hadronic physical quantity M (where $M = M_V$, f_{PS}, f_V, M_n or M_δ). As a first approximation, the dependence of M on the hadron's quark masses can be approximated by

$$Ma = A_M + B_M \sum_{q=1}^{Q} m_q a, \tag{10}$$

where the m_q are the masses of the constituent quarks, and $Q = 2, 3$ for mesons, baryons. This is the usual assumption of the quark model. In order to continue we need the additional assumption of PCAC

$$(M_{PS}a)^2 = D(m_1 a + m_2 a). \tag{11}$$

Combining eqs. 10 and 11 and eliminating the quark masses we have in the case of $M = M_V$,

$$M_V a = A_{M_V} + \frac{B_{M_V}}{D}(M_{PS}a)^2. \tag{12}$$

Assuming this remains valid from the simulation region down to (near-) zero quark masses, we can obtain a prediction for $M_\rho a$ and $(M_\pi a)^2$ as follows.

- On the $(M_V a\ , (M_{PS}a)^2)$ plane we impose the physical ratio $C_{ll} = M_\rho / M_\pi$. The intercept of this curve and the linear extrapolation of the simulated data defines $M_\rho a$ and $M_\pi a$ (only one independent).
- We now use the value of $M_\pi a$ determined above to read off the lattice meson decay constants, $(f_\pi a / Z_A)$ and $(f_\rho Z_V)^{-1}$ from the corresponding f_{PS} and f_V planes.

From Eq.(11) we immediately have

$$(M_{\eta_{ss}}a)^2 = 2(M_K a)^2 - (M_\pi a)^2, \tag{13}$$

where η_{ss} is the hypothetical pseudoscalar meson with quark content $s\overline{s}$ assuming no mixing with other states, for whose 'experimental' mass we have

$M_{\eta_{ss}} = 0.686\ GeV$. Using the lattice value of $M_{\eta_{ss}}a$, we can determine M_ϕ and $(f_\phi Z_V)^{-1}$ from Figs. 5 & 9. As a check of the assumption of PCAC and Eq. 10, we plot in Fig. 10 the lattice values of M_V/M_{K^*} against M_{PS}^2/M_K^2 together with their experimental values. The data lie on a straight line to remarkable accuracy.

For baryonic masses, the situation is more complicated. Eq.(10) can be written as:

$$\begin{aligned} M_n a &= A_{M_n} + B_{M_n}(m_1 a + m_2 a + m_3 a), \\ M_\delta a &= A_{M_\delta} + B_{M_\delta}(m_1 a + m_2 a + m_3 a). \end{aligned} \tag{14}$$

Combining these with eq. (11) leads to

$$\begin{aligned} M_N a &= A_{M_n} + \frac{B_{M_n}}{D}\left[\frac{3}{2}(M_\pi a)^2\right] \\ M_{\Lambda\Sigma} a &= A_{M_n} + \frac{B_{M_n}}{D}\left[(M_K a)^2 + \frac{1}{2}(M_\pi^2 a)^2\right] \\ M_\Xi a &= A_{M_n} + \frac{B_{M_n}}{D}\left[2(M_K a)^2 - \frac{1}{2}(M_\pi a)^2\right] \\ M_\Delta a &= A_{M_\delta} + \frac{B_{M_\delta}}{D}\left[\frac{3}{2}(M_\pi a)^2\right] \\ M_\Omega a &= A_{M_\delta} + \frac{B_{M_\delta}}{D}\left[3(M_K a)^2 - \frac{3}{2}(M_\pi a)^2\right]. \end{aligned}$$

where

$$M_{\Lambda\Sigma} = \frac{1}{4}M_\Sigma + \frac{3}{4}M_\Lambda \tag{15}$$

The baryonic masses can be extracted by fitting the data for $M_n a$ and $M_\delta a$ against $(M_{PS}a)^2$ to a straight line and using the values of $M_\pi a$ and $M_K a$ already determined, (see Figs. 6 and 7). Due to the limited number of K values, we do not attempt the fit to more complicated functions [17]. We have also checked that a quadratic fit does not give better χ^2. Our predictions of the initial 3 quantities which do not require any chiral extrapolation have then been extended to include the following quantities which do require chiral extrapolations and quark model considerations:

$$M_\rho, M_\phi, f_\pi/Z_A, (f_\rho Z_V)^{-1}, (f_\phi Z_V)^{-1}, M_N, M_{\Lambda\Sigma}, M_\Xi, M_\Delta \text{and} M_\Omega.$$

The method outlined above has the following properties:

- We use only the lattice physical planes and not the unphysical planes where

the $x-$axis is the quark mass $1/K$. These unphysical planes will only be required when we need to determine unphysical quantities such as the quark masses.
- This method allows us to fix the value of $M_{K^*}a$, and therefore a^{-1} without the need of any chiral extrapolation. It also enables us to determine f_K and f_{K^*} without any extrapolation.
- With the additional assumption of PCAC (Eq.(11)) and the quark model (Eq.(10)) we can derive the rest of the meson spectrum and decay constants, and the baryon spectrum.
- The conventional approach can be seen as the limit $C_{ll} \to \infty$ of this approach.

In the next section we use the above method to determine the physical quantities from the lattice simulations.

4 Results

This section briefly lists the results obtained using the method described in the previous section. Tables 3 - 10 contain the lattice data at each K value for $M_{PS}a$, M_Va, M_na, $M_\delta a$, $f_{PS}a/Z_A$ and $(f_VZ_V)^{-1}$ from the fits outlined is Section 2. Also listed are the K_c values (obtained using Eq.(11) with $m_q = 1/2(1/K_q - 1/K_c)$ and the chiral extrapolants using a linear fit with M_{PS}^2. All the mesonic and baryonic masses are also plotted in figs 10-12 and show a very good consistency, within the errors, among the various lattices. This shows that we observe a scaling behaviour in our data.

4.1 Hadron masses and decay constants

Using the method described in Sect. 3, the meson masses and decay constants (in lattice units) are displayed in Table 12 and 13. The inverse lattice spacing, a^{-1}, obtained from the experimental values is displayed in Table 11.
Similarly the baryon masses, are displayed in Table 14. Again, for comparison, the a^{-1} values obtained using these masses are shown in Table 11. Note that all errors quoted in Tables 12, 13 and 14 are statistical only. In Tables 15 - 17, a listing is given of the lattice predictions of the mass spectrum and decay constants from C60 - C64. The scale was set from the K^* mass.

Comparing the clover meson masses at $\beta = 6.2$ from lattices C62a, C62b and the UKQCD results [16] in fig. 13, we find very good agreement with UKQCD for Lattice C62a. For C62b, while we find unexpectedly larger fluctuations in the comparison, we seem to get a somewhat lower mass; there may be some

residual finite size effects in the vector meson mass, even though one would rather expect a higher mass in this case. This problem may also be present for the $\beta = 6.4$ data for which the physical volume is the same as in C62b. Further investigation at larger lattice sizes is necessary to make the situation clearer. At $\beta = 6.0$ we can also compare our Wilson data with [25], [11] and [18], see Table 4 and fig. 14. The agreement is very good for the pseudoscalar data for which we have K values in common. Our data for the vector mass at the lightest quark mass is slightly higher. We do not have a clear explanation for this. We only note that if we had fitted our data in the t region in the interval $11 - 21$ as done in fig. 2 of ref. [18] our value for the vector mass would have been $M_V = 0.427(4)$ which is in much better agreement with their value. On the other hand, for the baryon data, we find very good agreement with the old APE [25] data, while we find slightly higher values and larger fluctuations when comparing with JLQCD [11] and LANL [18] data as shown in fig. 15.

As can be seen from Tables 15 - 16, there is good consistency of the physical predictions between the different simulations to within statistical errors. Considering the fact that the errors shown in Tables 15 - 16 are statistical only, and that these can often be underestimated [11], the agreement is remarkable.

To compare the lattice decay constants with the experimental ones, we have used a 'boosted' one-loop form of the renormalisation constants [19] - [21]:

$$\begin{aligned} \text{Wilson action} \quad Z_A &= 1 - 0.134 g^2_{\overline{MS}} \\ Z_V &= 1 - 0.174 g^2_{\overline{MS}} \\ \text{Clover action} \quad Z_A &= 1 - 0.0177 g^2_{\overline{MS}} \\ Z_V &= 1 - 0.10 g^2_{\overline{MS}} \end{aligned}$$

where $g^2_{\overline{MS}} = 6/\beta_{\overline{MS}}$, with [23] - [24]

$$\beta_{\overline{MS}} = < U_{plaq} > \beta + 0.15. \tag{16}$$

The results are shown in Table 17 and figs. 16 & 19. For the ratio f_{PS}/M_V in figs. 16-figs. 17, we see again a global consistency of our different data both for Wilson and the SW-Clover action. The UKQCD data [16], also reported in fig.17, with the same renormalization decay constant Z_A disagree with ours for two of the three points where the comparison is possible. For the third point there is agreement but within much larger error bars. We do not see a strong a dependence for either actions comparing lattices at different β (C60, C62a and W60, W62a). This confirms statements made in Sect. 2 about the statistical presence of scaling in our data. The experimental points do lie quite well in the band extrapolated/interpolated from the lattice data.

The values of the pseudoscalar decay constants in Table 17 show larger deviations from the experimental data than the ratio f_{PS}/M_V. It is clear that a cancellation of systematic error occurs in this ratio. Still there is an agreement within 1.5 standard deviations with the experimental data apart from the W60 value which is quite high. In particular it is higher than the value obtained for the Wilson action at $\beta = 6$ in ref. [22]. There the authors use different renormalization schemes than the one used here but the discrepancy is too large to be attributed to this.

The situation is more delicate for the vector decay constant for which a dependence on the volume and a^{-1} may be present but with our data it would be difficult to disentangle the two effects. In particular in figs. 18, 19 and Table 17 the values for C62a and C62b (SW-Clover on different physical volumes), C62a and W62a (SW-Clover and Wilson with the same physical volume), W60 and W62a (Wilson with the same physical volume but different values of β) and C60 and C62a (SW-Clover on the same volume and different β) seem to show this problem. The extrapolated values for $1/f_V$ suffer very much due to these effects. The 'strange' vector decay constants seem to be slightly more stable also because no extrapolation is needed.

4.2 Meson Dispersion relations

For all the lattices except for W62b the non-zero momentum meson correlation functions were also computed. We can study discretization errors and finite volume effects testing which dispersion relation is best verified from data. We have tested the following dispersion relations

$$E^2 = p^2 + M^2 \ , \tag{17}$$

$$\sinh^2(\frac{E}{4}) = \sin^2(\frac{p}{4}) + \sinh^2(\frac{M}{4}) \ , \tag{18}$$

$$\sinh^2(\frac{E}{2}) = \sin^2(\frac{p}{2}) + \sinh^2(\frac{M}{2}) \ , \tag{19}$$

$$\sinh^2(E) = \sin^2(p) + \sinh^2 M \ , \tag{20}$$

where (17) is the continuum relation, while the others are lattice dispersion relations from different choices of lattice action. $M = E(\vec{p} = 0)$ is the mass. From the lattice we have extracted the energy $E(\vec{p})$ of the states fitting the non-zero momentum correlation functions with a *cosh* function. The results we obtained for $E(\vec{p})$ for pseudoscalar and vector mesons are reported in Table 18. We see only small differences among the various dispersion relations for the quark masses we have simulated, but eq. (19) seems to be favoured [2]. This is consistent with the conclusion of ref. [18] which refers however to much larger quark masses.

4.3 Strange Quark Mass

Lattice QCD is in principle able to predict the mass of any quark by fixing to its experimental value the mass of a hadron containing a quark with the same flavour. The 'bare' lattice quark mass $m(a)$ can be extracted directly from lattice simulations and can be related to the continuum mass $m^{\overline{MS}}(\mu)$ renormalized in the minimal-subtraction dimensional scheme through a well-defined perturbative procedure [26] - [28] . Following ref. [29]

$$m^{\overline{MS}}(\mu) = Z_m^{\overline{MS}}(\mu a) m(a)$$

where $m(a)$ is the bare lattice quark mass related to the hopping parameter as

$$m(a)a = \frac{1}{2}(\frac{1}{K} \ - \ \frac{1}{K_c}) \ . \tag{21}$$

and $Z_m^{\overline{MS}}(\mu a)$ is the mass renormalization constant at scale μ which we choose to be 2 GeV. The hopping parameters and the strange quark masses reported in Tables 19 and 20 are extracted using the eq. (21) and (11) from the lattice values $M_\pi a$ and $M_K a$. The error on $m^{\overline{MS}}(\mu)$ is estimated as in ref. [29] taking into account the spread due to different definitions of the strong coupling constant. This leads to somewhat larger errors for the Wilson data than for the Clover ones due to the smaller fluctuation of the different renormalization constants in the improved case. There is a good consistency among the values coming from the different lattices. Fig. 20 shows that we do not see any dependence on a within the errors in the Wilson data and a mild tendency in the clover data to decrease with increasing β. We therefore conclude that any $O(a)$ effects present are beneath the level of statistics, and/or hidden among finite volume effects. We then extract the average value of the strange quark mass without any extrapolation and get:

$$m_s^{\overline{MS}}(\mu = 2GeV) = 122 \pm 20 MeV$$

which is in agreement with the result of ref. [29]. It is also compatible with the value $m_s^{\overline{MS}}(\mu = 2GeV) = 90 \pm 20 \ MeV$ of ref. [30], but one should take into account that this value comes from an analysis on various Wilson and Staggered lattices at different values of β and an extrapolation in a. The quark masses can also be extracted from the Ward identity for the axial vector current. A full analysis of the light quarks masses from both methods will be presented in a forthcoming paper.

4.4 J value(s)

In this section we analyze the effect of the quenched approximation using the J variables first proposed for mesons by Lacock and Michael [13].
In the spirit of the Maiani-Martinelli proposal [14][16] to use $(M_{K^*}-M_\rho)/(M_K^2-M_\pi^2)$ as an independent way to determine the lattice scale and avoiding the chiral extrapolation as described in section 3, Lacock and Michael proposed that

$$J = M_{K^*}\frac{dM_V}{dM_{PS}^2}, \tag{22}$$

be computed on the lattice and compared with experimental values. J is a combination of parameters which is independent of a and K and which does not require any chiral extrapolation to the chiral limit. We use the experimental values of the meson masses reported in Table 15 to determine the experimental values of J. This gives the dimensionless value reported in Table 21.
Using the method described in section 3 it is very easy to extract the J value for mesons. The results we have obtained are reported in the Table 21. The lattice values for J are significantly different to the experimental value and one can see a dependence on β but as discussed before a volume effect may be present on C62b, W64 and C64 which prevents a clear conclusion. The disagreement between the data and the experimental value of J is also evident in fig. 10. It is easy to see that, in the plane of fig. 10, the J value is proportional to the slope of the line through the experimental data which is clearly different to the slope of the lattice data.

As well as defining the quantity J for the meson sector, a corresponding quantity for the nucleon and delta sector can be introduced. This can be viewed as the slope of the data in figs. 11, 12. While the data is noisy, it is likely that the lattice data also underestimates the slope of the experimental points in these plots.

5 Conclusions

We have analyzed a large set of data on lattices of different lattice spacing and lattice sizes with both the Wilson and SW-Clover actions. These simulations were not originally performed for a hadron spectrum study, hence the relatively large values for the light quark masses. To overcome potential problems with the chiral extrapolation, a new technique of obtaining lattice predictions without any extrapolation in the quark mass was developed.

In the β range studied, we conclude that there is no statistical evidence for an a dependence in the hadron masses or for the pseudoscalar decay constants. Our data agrees with the experimental data to within $\sim 5\%$ for mesonic masses and $\sim 10\% - 15\%$ for baryonic masses and the pseudoscalar decay constants. A larger deviation is present for the vector decay constants which, in our opinion, deserve a more careful study at larger volumes and β. The effects of finite size, if present, are within the statistical errors of our data.

We obtain for the strange quark mass $m_s^{\overline{MS}}(\mu = 2GeV) = 122 \pm 20\ MeV$ without seeing any clear a dependence. The meson dispersion relations and the quantity J were also studied.

We believe that the lattice results at $\beta \geq 6$ are quite stable and show a scaling behaviour, within current statistical errors.

Acknowledgements

We wish to thank the APE collaboration for allowing us to use the lattice correlation functions presented here. We warmly thank R. Gupta, V. Lubicz, G. Martinelli, G. Parisi, S. Sharpe and A. Vladikas for useful discussions. We also thank E. Franco for providing us the code for the computation of the renormalization constants of vector and axial currents. This work was partially supported by the EC Contract 'Computational Particle Physics' CHRX-CT92-0051, and by the EC Human Capital and Mobility Program, contracts ERBCHBICT941462 and ERBCHBGCT940665. V.G. wishes to thank the Dipartimento di Fisica "G. Marconi" of the Università di Roma "La Sapienza" for its hospitality, and acknowledges partial support by CICYT under grant number AEN-96/1718.

References

[1] M. Crisafulli et al., Phys. Lett. B 369 (1996) 325.

[2] APE Collaboration (As. Abada et al.) Phys. Lett. B 365 (1996) 275.

[3] APE Collaboration (C.R. Allton et al.), Phys. Lett. B 345 (1995) 513.

[4] APE Collaboration (C.R. Allton et al.), Nucl. Phys. B (Proc. Suppl.) 34 (1994) 456.

[5] APE Collaboration (C.R. Allton et al.), Nucl. Phys. B (Proc. Suppl.) 34 (1994) 360.

[6] APE Collaboration, Work in progress

[7] APE Collaboration (C.R. Allton et al.), Phys. Lett. B 326 (1994) 295.

[8] APE Collaboration (P. Bacilieri et al.), Nucl. Phys. B 317 (1989) 509.

[9] C. R. Allton, Nucl. Phys. B 437 (1995) 641.

[10] C. R. Allton, hep-lat/9610016.

[11] JLQCD Collaboration (S. Aoki et al.), Nucl. Phys. B (Proc. Suppl.) 47 (1996) 354.

[12] S. R. Sharpe, Phys. Rev. D 46 (1992) 3146.

[13] UKQCD Collaboration (P. Lacock et al.), Phys. Rev. D 52 (1995) 5213.

[14] L. Maiani and G. Martinelli, Phys. Lett. B 178 (1986) 265.

[15] F. Butler et al., Nucl. Phys. B 430 (1994) 179.

[16] UKQCD Collaboration (C.R. Allton et al.), Phys. Rev. D 49 (1994) 474.

[17] S. Gottlieb, review talk at LATTICE 96, St. Louis, USA, June 1996, hep-lat/9608107;
M. Göckeler et al., DESY 96-173, hep-lat/9609008;
S. R. Sharpe, plenary talk at LATTICE 96, St. Louis, USA, June 1996, hep-lat/9609029.

[18] T. Bhattacharya, R. Gupta, G. Kilcup and S. Sharpe, Phys. Rev. D 53 (1996) 6486.

[19] G. Martinelli and Y.C. Zhang, Phys. Lett. B 123 (1983) 433.

[20] E. Gabrielli et al., Nucl. Phys. B 362 (1991) 475.

[21] A. Borrelli, C. Pittori, R. Frezzotti and E. Gabrielli, Nucl. Phys. B 409 (1993) 382.

[22] R. Gupta and T. Bhattacharya, Phys. Rev. D 54 (1996) 1155.

[23] A. X. El-Khadra et al, Phys. Rev. Lett. 69(1992) 729.

[24] G. Peter Lepage and Paul B. Mackenzie, Phys. Rev. D 48 (1993) 2250.

[25] APE Collaboration (S. Cabasino et al.), Phys. Lett. B 258(1991) 195.

[26] A. Gonzalez Arroyo, G. Martinelli and F. J. Yndurain, Phys. Lett. B 117 (1982) 437.

[27] H.W. Hamber and C.M. Wu, Phys. Lett. B 136 (1984) 255.

[28] M. Bochicchio et al., Nucl. Phys. B 262 (1985) 331.

[29] C.R. Allton et al., Nucl. Phys. B 431 (1994) 667.

[30] R. Gupta and T. Bhattacharya, hep-lat/9605039.

Table 3
Hadron masses and meson decay constants versus the hopping parameter for Lattice C60.

K	$M_{PS}a$	$M_V a$	$M_n a$	$M_\delta a$	$f_{PS}a/Z_A$	$1/(f_V Z_V)$
0.1425	0.439(1)	0.549(5)	0.833(9)	0.90(2)	0.095(2)	0.324(9)
0.1432	0.382(1)	0.512(7)	0.76(1)	0.84(3)	0.089(2)	0.34(1)
0.1440	0.308(1)	0.48(1)	0.69(1)	0.78(5)	0.082(3)	0.38(2)
0.14549(2)	-	0.40(2)	0.54(2)	0.65(7)	0.069(4)	0.43(4)

Table 4
As in Table 3 for Lattice W60.

K	$M_{PS}a$	$M_V a$	$M_n a$	$M_\delta a$	$f_{PS}a/Z_A$	$1/(f_V Z_V)$
0.1530	0.423(1)	0.508(3)	0.801(6)	0.864(8)	0.114(2)	0.391(6)
0.1540	0.364(1)	0.468(4)	0.729(7)	0.81(1)	0.108(2)	0.420(8)
0.1550	0.298(1)	0.431(6)	0.66(1)	0.75(2)	0.100(2)	0.46(1)
0.15703(2)	-	0.353(9)	0.52(1)	0.64(3)	0.087(3)	0.52(2)

Table 5
As in Table 3 for Lattice C62a.

K	$M_{PS}a$	$M_V a$	$M_n a$	$M_\delta a$	$f_{PS}a/Z_A$	$1/(f_V Z_V)$
0.14144	0.297(1)	0.386(3)	0.586(5)	-	0.066(1)	0.310(6)
0.14184	0.258(1)	0.362(5)	0.542(8)	-	0.062(2)	0.326(9)
0.14224	0.215(1)	0.34(1)	0.50(1)	-	0.057(2)	0.35(2)
0.14264	0.162(2)	0.34(3)	0.46(4)	-	0.052(3)	0.40(6)
0.14315(1)	-	0.29(2)	0.40(3)	-	0.046(3)	0.39(3)

Table 6
As in Table 3 for Lattice W62a.

K	$M_{PS}a$	$M_V a$	$M_n a$	$M_\delta a$	$f_{PS}a/Z_A$	$1/(f_V Z_V)$
0.1510	0.289(1)	0.366(2)	0.566(4)	-	0.080(1)	0.381(6)
0.1515	0.254(1)	0.343(3)	0.525(6)	-	0.075(1)	0.401(7)
0.1520	0.215(1)	0.321(5)	0.48(1)	-	0.070(2)	0.42(1)
0.1526	0.158(1)	0.29(1)	0.45(3)	-	0.062(2)	0.45(3)
0.15329(1)	-	0.26(1)	0.38(2)	-	0.056(2)	0.48(2)

Table 7
As in Table 3 for Lattice C62b.

K	$M_{PS}a$	$M_V a$	$M_n a$	$M_\delta a$	$f_{PS}a/Z_A$	$1/(f_V Z_V)$
0.14144	0.294(3)	0.378(6)	0.59(2)	0.68(1)	0.066(2)	0.29(1)
0.14190	0.249(3)	0.34(1)	0.53(2)	0.65(2)	0.061(2)	0.30(2)
0.14244	0.186(4)	0.30(3)	0.43(5)	0.57(4)	0.055(3)	0.29(4)
0.14312(4)	-	0.25(3)	0.35(7)	0.53(6)	0.048(4)	0.30(4)

Table 8
As in Table 3 for Lattice W62b.

K	$M_{PS}a$	$M_V a$	$M_n a$	$M_\delta a$	$f_{PS}a/Z_A$	$1/(f_V Z_V)$
0.1510	0.291(1)	0.370(3)	0.576(7)	0.618(7)	0.079(2)	0.390(9)
0.1520	0.217(1)	0.323(7)	0.50(2)	0.56(2)	0.069(2)	0.43(2)
0.1526	0.160(2)	0.29(1)	0.42(6)	0.55(4)	0.062(2)	0.46(3)
0.15330(2)	-	0.26(1)	0.38(6)	0.49(4)	0.055(2)	0.49(3)

Table 9
As in Table 3 for Lattice W64.

K	$M_{PS}a$	$M_V a$	$M_n a$	$M_\delta a$	$f_{PS}a/Z_A$	$1/(f_V Z_V)$
0.1488	0.235(1)	0.289(2)	0.461(4)	0.499(7)	0.0609(9)	0.333(4)
0.1492	0.205(2)	0.266(3)	0.423(5)	0.47(1)	0.0573(9)	0.346(6)
0.1496	0.172(2)	0.242(4)	0.38(1)	0.42(2)	0.053(1)	0.359(8)
0.1500	0.136(3)	0.22(1)	0.33(3)	0.36(4)	0.048(2)	0.38(2)
0.15058(3)	-	0.188(9)	0.28(2)	0.33(4)	0.043(2)	0.39(2)

Table 10
As in Table 3 for Lattice C64.

K	$M_{PS}a$	$M_V a$	$M_n a$	$M_\delta a$	$f_{PS}a/Z_A$	$1/(f_V Z_V)$
0.1400	0.249(1)	0.306(2)	0.484(4)	0.52(1)	0.0524(9)	0.269(5)
0.1403	0.220(1)	0.283(3)	0.446(6)	0.49(1)	0.049(1)	0.276(6)
0.1406	0.188(2)	0.259(5)	0.40(1)	0.44(2)	0.046(1)	0.281(8)
0.1409	0.152(3)	0.23(1)	0.34(2)	0.37(4)	0.042(1)	0.29(2)
0.14143(3)	-	0.19(1)	0.29(2)	0.32(5)	0.037(2)	0.30(2)

Table 11
Values of a^{-1} in GeV from different observables for all lattices. The values of $a^{-1}_{K^*}$ (shown in boldface) are taken as our preferred estimate of the inverse lattice spacing.

	C60	W60	C62a	W62a	C62b	W62b	W64	C64
a^{-1}_{ρ}	1.88(9)	2.15(5)	2.6(2)	2.9(1)	3.0(3)	2.9(2)	4.0(2)	3.9(2)
$a^{-1}_{K^*}$	**1.98(8)**	**2.26(5)**	**2.7(1)**	**3.00(9)**	**3.0(3)**	**3.0(1)**	**4.1(2)**	**4.0(2)**
$a^{-1}_{\eta_{ss}}$	1.98(8)	2.26(5)	2.7(1)	3.00(9)	3.0(3)	3.0(1)	4.2(2)	4.0(2)
a^{-1}_{ϕ}	2.06(7)	2.35(5)	2.8(1)	3.10(8)	3.1(3)	3.1(1)	4.3(2)	4.1(2)
a^{-1}_{N}	1.70(6)	1.79(5)	2.3(1)	2.4(1)	2.7(5)	2.4(3)	3.2(2)	3.2(2)
$a^{-1}_{\Lambda\Sigma}$	1.86(6)	1.99(4)	2.5(1)	2.7(1)	2.8(4)	2.7(3)	3.6(2)	3.5(2)
a^{-1}_{Ξ}	1.98(6)	2.13(4)	2.68(8)	2.84(8)	2.9(4)	2.8(2)	3.8(2)	3.7(2)
a^{-1}_{Δ}	1.9(2)	1.90(8)	-	-	2.3(2)	2.5(2)	3.7(4)	3.8(5)
a^{-1}_{Ω}	2.07(9)	2.21(6)	-	-	2.7(1)	2.9(1)	4.0(2)	4.0(3)
$a^{-1}_{f_\pi}$	1.9(1)	1.90(7)	2.9(2)	2.9(1)	2.8(2)	2.9(1)	3.7(2)	3.6(2)
$a^{-1}_{f_K}$	2.11(8)	2.16(6)	3.0(1)	3.1(1)	3.1(2)	3.17(9)	4.1(1)	4.0(1)

Table 12
Extrapolated/interpolated meson masses in lattice units for all lattices.

	$M_\rho a$	$M_{K^*} a$	$M_{\eta_{ss}} a$	$M_\phi a$
C60	0.41(2)	0.45(2)	0.35(1)	0.49(2)
W60	0.358(9)	0.395(9)	0.303(7)	0.433(9)
C62a	0.30(2)	0.33(2)	0.25(1)	0.36(1)
W62a	0.27(1)	0.298(9)	0.229(7)	0.329(9)
C62b	0.26(3)	0.29(3)	0.23(2)	0.33(3)
W62b	0.26(1)	0.30(1)	0.23(1)	0.33(1)
W64	0.192(8)	0.215(8)	0.165(6)	0.239(8)
C64	0.20(1)	0.22(1)	0.171(8)	0.25(1)

Table 13
Extrapolated/interpolated meson decay constants for all lattices.

	$f_\pi a/(Z_A m_\rho a)$	$1/(f_\rho Z_V)$	$f_K a/(Z_A m_{K^*} a)$	$1/(f_{K^*} Z_V)$	$1/(f_\phi Z_V)$	f_K/f_π
C60	0.17(1)	0.42(3)	0.172(9)	0.39(2)	0.36(1)	1.11(2)
W60	0.25(1)	0.51(2)	0.239(8)	0.48(2)	0.45(1)	1.08(1)
C62a	0.16(1)	0.39(3)	0.164(9)	0.36(2)	0.332(8)	1.15(3)
W62a	0.21(1)	0.47(2)	0.214(8)	0.45(1)	0.417(8)	1.13(1)
C62b	0.19(3)	0.30(4)	0.18(2)	0.30(3)	0.30(2)	1.10(3)
W62b	0.21(1)	0.49(3)	0.21(1)	0.46(2)	0.43(1)	1.12(2)
W64	0.23(2)	0.39(2)	0.22(1)	0.38(1)	0.363(8)	1.10(2)
C64	0.19(1)	0.30(2)	0.18(1)	0.29(1)	0.284(9)	1.10(1)

Table 14
Extrapolated/interpolated baryon masses in lattice units for all lattices.

	$M_N a$	$M_{\Lambda\Sigma} a$	$M_\Xi a$	$M_\Delta a$	$M_\Omega a$
C60	0.55(2)	0.61(2)	0.67(2)	0.66(6)	0.81(3)
W60	0.53(1)	0.57(1)	0.62(1)	0.65(3)	0.76(2)
C62a	0.41(3)	0.45(2)	0.49(1)	-	-
W62a	0.39(2)	0.43(2)	0.46(1)	-	-
C62b	0.35(7)	0.40(6)	0.45(5)	0.53(6)	0.62(2)
W62b	0.39(5)	0.43(5)	0.46(4)	0.50(4)	0.57(2)
W64	0.29(2)	0.32(2)	0.35(1)	0.34(4)	0.42(2)
C64	0.29(2)	0.32(2)	0.35(2)	0.33(5)	0.42(3)

Table 15
Predicted meson masses in GeV for all lattices, using the scale from M_{K^*}.

	M_ρ	$M_{\eta_{ss}}$	M_ϕ
Exper.	0.770	0.686 (see text)	1.019
C60	0.809(7)	0.6849(3)	0.977(7)
W60	0.808(3)	0.6849(1)	0.978(3)
C62a	0.81(1)	0.6849(5)	0.98(1)
W62a	0.803(6)	0.6851(2)	0.984(6)
C62b	0.79(1)	0.6856(5)	1.00(1)
W62b	0.797(7)	0.6853(3)	0.989(7)
W64	0.796(4)	0.6853(2)	0.990(4)
C64	0.792(4)	0.6855(2)	0.994(4)

Table 16
Predicted baryon masses in GeV for all lattices, using the scale from M_{K^*}.

	M_N	$M_{\Lambda\Sigma}$	M_Ξ	M_Δ	M_Ω
Exper.	0.9389	1.135	1.3181	1.232	1.6724
C60	1.09(5)	1.21(4)	1.32(4)	1.3(1)	1.60(9)
W60	1.19(5)	1.29(4)	1.40(4)	1.46(7)	1.71(4)
C62a	1.1(1)	1.22(8)	1.34(7)	-	-
W62a	1.17(7)	1.28(6)	1.39(5)	-	-
C62b	1.1(2)	1.2(2)	1.4(1)	1.6(3)	1.9(2)
W62b	1.2(1)	1.3(1)	1.40(9)	1.50(9)	1.72(5)
W64	1.21(9)	1.32(8)	1.43(6)	1.4(2)	1.72(9)
C64	1.2(1)	1.29(8)	1.41(7)	1.3(2)	1.7(1)

Table 17
Predicted meson decay constants for all lattices, using the scale from M_{K^*}.

	f_π (GeV)	$\frac{1}{f_\rho}$	f_K (GeV)	$\frac{1}{f_{K^*}}$	$\frac{1}{f_\phi}$
Exper.	0.1307	0.28	0.1598		0.23
C60	0.134(9)	0.35(3)	0.149(8)	0.33(2)	0.30(1)
W60	0.155(7)	0.37(2)	0.167(6)	0.35(1)	0.324(8)
C62a	0.124(9)	0.33(3)	0.143(8)	0.30(2)	0.281(7)
W62a	0.135(6)	0.35(2)	0.153(5)	0.33(1)	0.307(6)
C62b	0.14(2)	0.26(4)	0.16(2)	0.25(3)	0.25(2)
W62b	0.135(8)	0.36(2)	0.152(7)	0.34(2)	0.315(9)
W64	0.147(9)	0.29(1)	0.161(8)	0.283(9)	0.272(6)
C64	0.144(9)	0.25(1)	0.158(8)	0.25(1)	0.243(8)

Table 18
Values of $E(\vec{p})$ for mesons with non-zero momentum versus the hopping parameter.

	K	$p^2=1$	$p^2=2$	$p^2=3$	$p^2=1$	$p^2=2$	$p^2=3$
C60	0.1425	0.567(4)	0.67(1)	0.73(3)	0.654(4)	0.751(8)	0.82(1)
	0.1432	0.526(6)	0.63(2)	0.68(4)	0.625(6)	0.73(1)	0.78(1)
	0.1440	0.479(9)	0.57(4)	0.60(8)	0.60(1)	0.70(2)	0.70(2)
W60	0.1530	0.554(5)	0.66(1)	0.73(2)	0.621(4)	0.716(7)	0.79(1)
	0.1540	0.513(7)	0.62(2)	0.68(4)	0.591(6)	0.692(9)	0.75(2)
	0.1550	0.47(1)	0.58(3)	0.62(7)	0.566(8)	0.67(2)	0.69(3)
C62a	0.14144	0.399(3)	0.479(6)	0.53(2)	0.476(3)	0.557(4)	0.618(8)
	0.14184	0.371(4)	0.455(9)	0.51(4)	0.455(3)	0.543(7)	0.60(1)
	0.14224	0.340(7)	0.43(1)	0.50(7)	0.436(5)	0.54(1)	0.59(2)
	0.14264	0.30(1)	0.40(3)	-	0.42(1)	0.56(3)	0.55(3)
W62a	0.1510	0.395(3)	0.479(6)	0.52(2)	0.459(2)	0.541(3)	0.605(7)
	0.1515	0.369(3)	0.459(9)	0.50(3)	0.440(3)	0.528(5)	0.592(9)
	0.1520	0.343(5)	0.44(1)	0.48(5)	0.423(3)	0.518(8)	0.58(1)
	0.1526	0.31(1)	0.41(3)	0.5(1)	0.404(6)	0.53(2)	0.54(3)
C62b	0.14144	0.48(1)	0.60(3)	-	0.536(7)	0.66(2)	0.77(4)
	0.14190	0.46(2)	0.56(4)	-	0.53(1)	0.64(3)	0.77(5)
	0.14244	0.42(6)	0.48(7)	-	0.53(3)	0.63(5)	0.76(8)
W62b	-	-	-	-	-	-	-
W64	0.1488	0.363(6)	0.47(2)	-	0.406(4)	0.50(1)	-
	0.1492	0.35(1)	0.46(4)	-	0.394(5)	0.50(2)	-
	0.1496	0.33(2)	0.46(8)	-	0.385(8)	0.51(4)	-
	0.1500	0.33(5)	0.4(2)	-	0.38(2)	0.6(1)	-
C64	0.1400	0.371(6)	0.49(2)	-	0.419(4)	0.51(1)	-
	0.1403	0.36(1)	0.49(4)	-	0.406(5)	0.51(2)	-
	0.1406	0.34(2)	0.50(8)	-	0.393(8)	0.52(5)	-
	0.1409	0.33(4)	0.5(2)	-	0.38(1)	0.6(2)	-

Table 19
Values for K_c, K_l and K_s for all lattices.

	K_c	K_l	K_s
C60	0.14549(2)	0.14540(2)	0.1436(1)
W60	0.15703(2)	0.15693(2)	0.15492(9)
C62a	0.14315(1)	0.14310(2)	0.1419(1)
W62a	0.15329(1)	0.15322(2)	0.15184(9)
C62b	0.14312(4)	0.14308(4)	0.1421(2)
W62b	0.15330(2)	0.15323(2)	0.1519(1)
W64	0.15058(3)	0.15054(3)	0.14969(8)
C64	0.14143(3)	0.14140(3)	0.14074(7)

Table 20
Values for the lattice strange lattice quark masses for all lattices and the corresponding $\overline{MS}$ values at NLO, both in MeV.

	$m_s(a)$	$m_s^{\overline{MS}}(\mu = 2\ GeV)$
C60	89(3)	120(10)
W60	98(2)	130(20)
C62a	83(4)	120(10)
W62a	93(3)	130(10)
C62b	75(6)	110(10)
W62b	92(4)	130(20)
W64	82(3)	120(10)
C64	69(3)	100(10)

Table 21
Predicted values of J for all lattices.

	J
Exper.	0.48
C60	0.34(3)
W60	0.34(1)
C62a	0.34(5)
W62a	0.36(2)
C62b	0.42(5)
W62b	0.38(3)
W64	0.39(2)
C64	0.40(2)

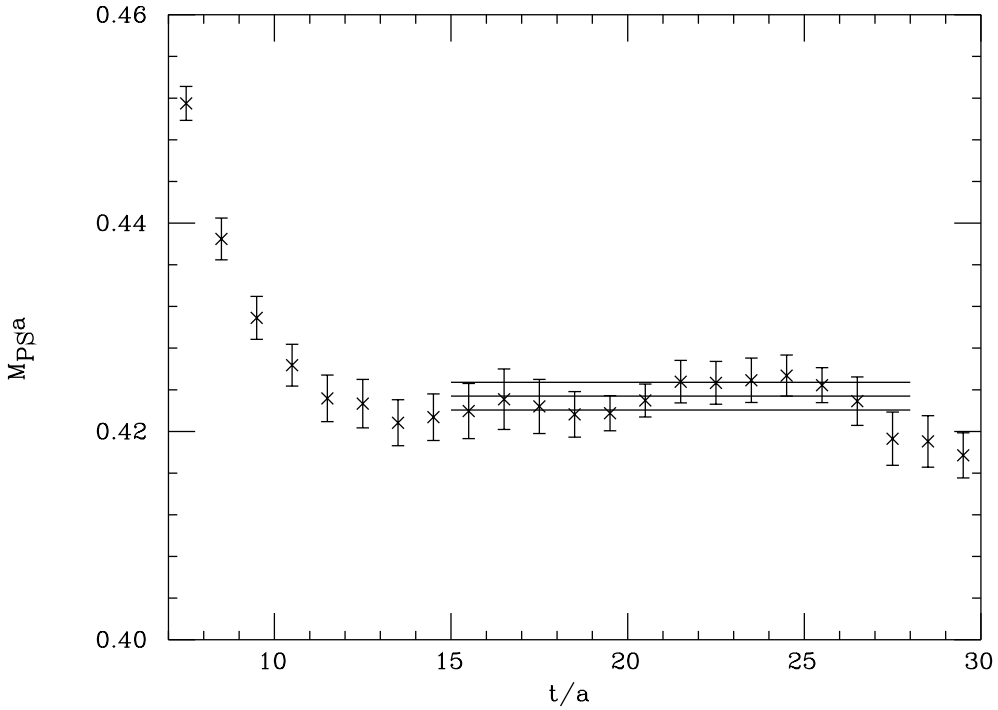

Fig. 1. Effective pseudoscalar mass M_{PS} in lattice units versus time for lattice W60 and $K = 0.1530$. Dashed lines show the fitted value and its error in the chosen time interval.

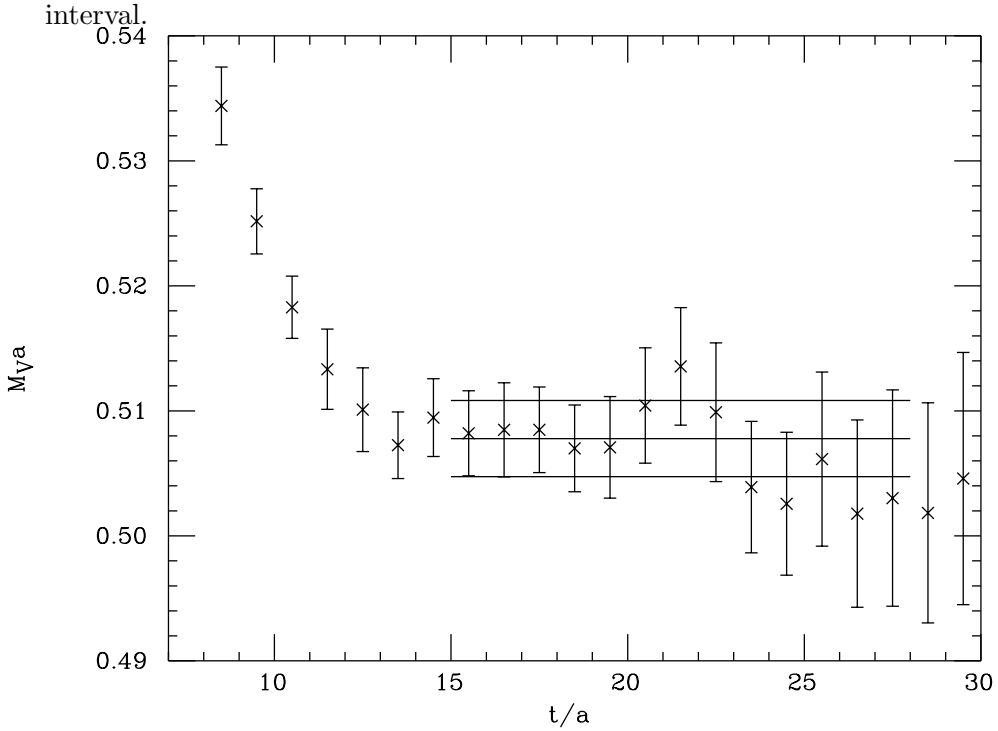

Fig. 2. As in fig. 1 for the vector meson mass M_V.

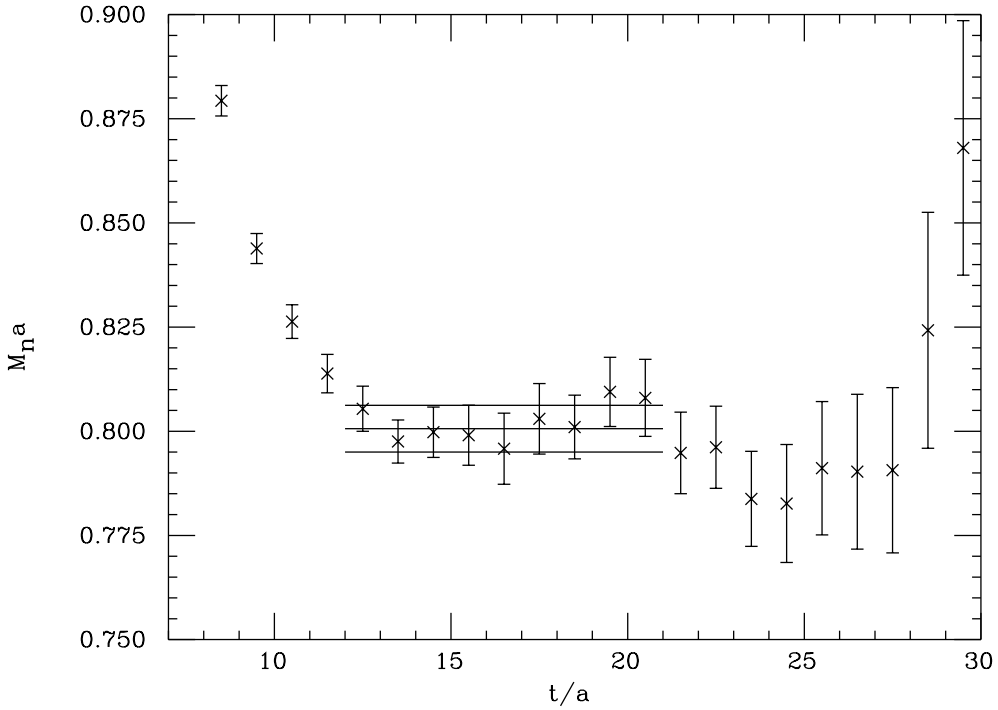

Fig. 3. As in fig. 1 for the nucleon mass M_n.

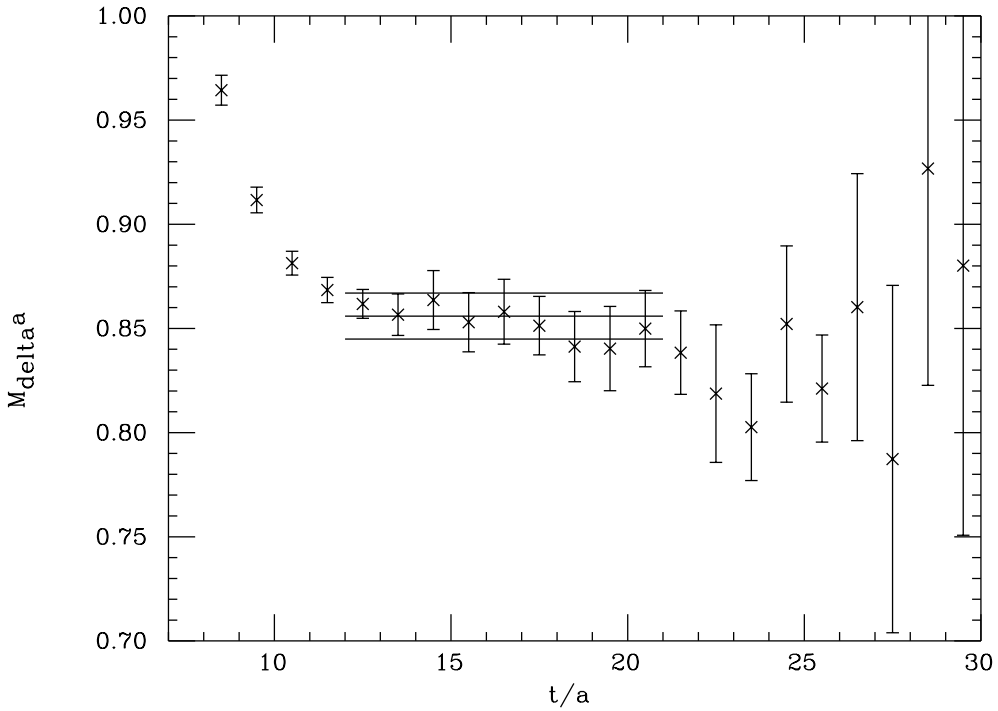

Fig. 4. As in fig. 1 for delta mass M_δ.

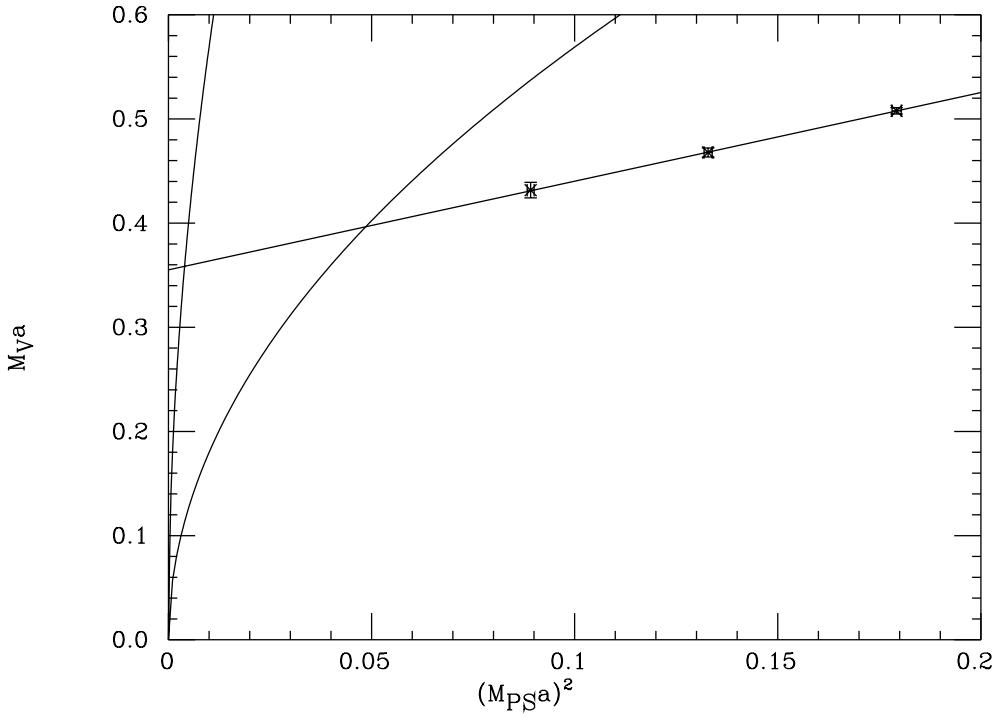

Fig. 5. Values of M_V versus M_{PS}^2 in lattice units and the fitting line for W60. The curves represent the equations $M_V a = C\sqrt{(M_{PS}a)^2}$ with $C = C_{ll}$ (leftmost) and $C = C_{sl}$ (rightmost) defined in section 3.

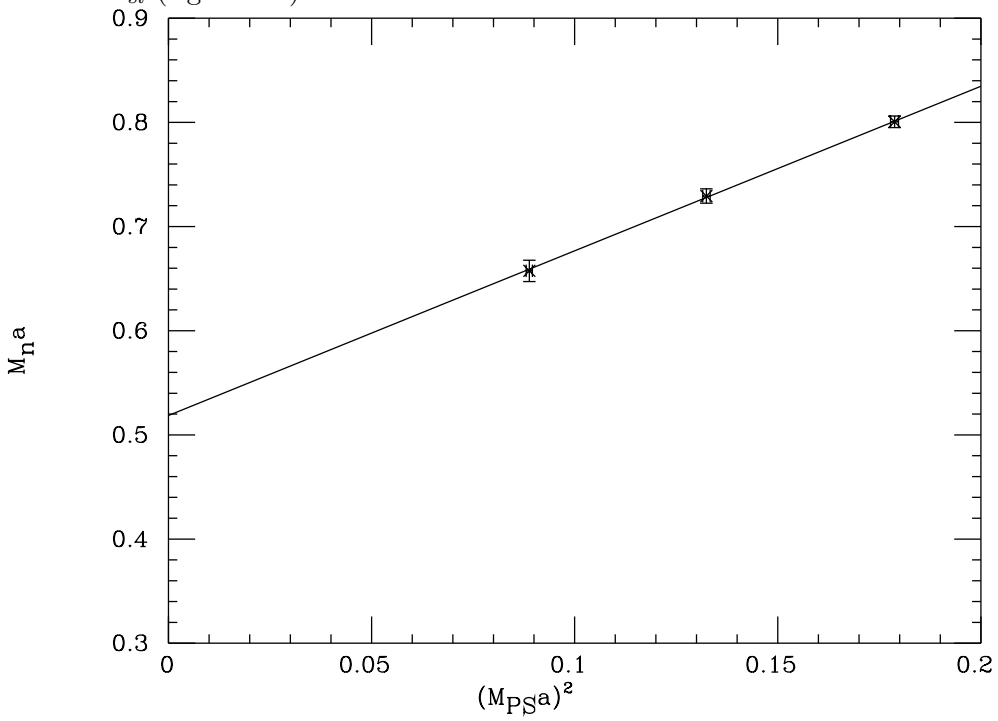

Fig. 6. Values of M_n versus M_{PS}^2 in lattice units and the fitting line for W60.

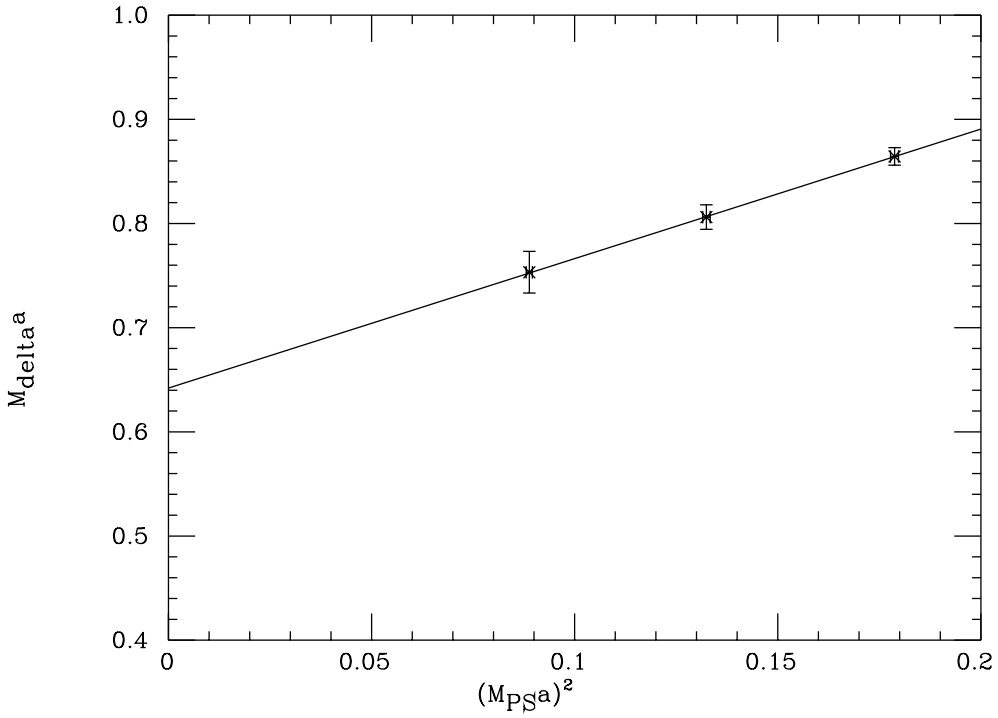

Fig. 7. As in fig. 6 for M_δ.

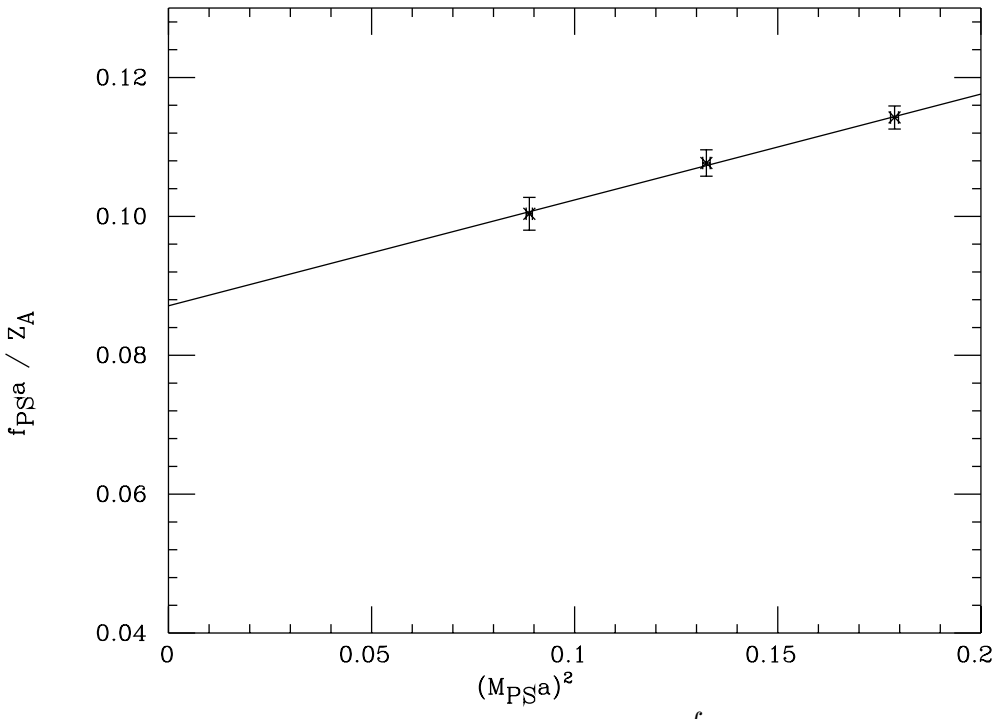

Fig. 8. As in fig. 6 for $\frac{f_{PS}}{Z_A}$.

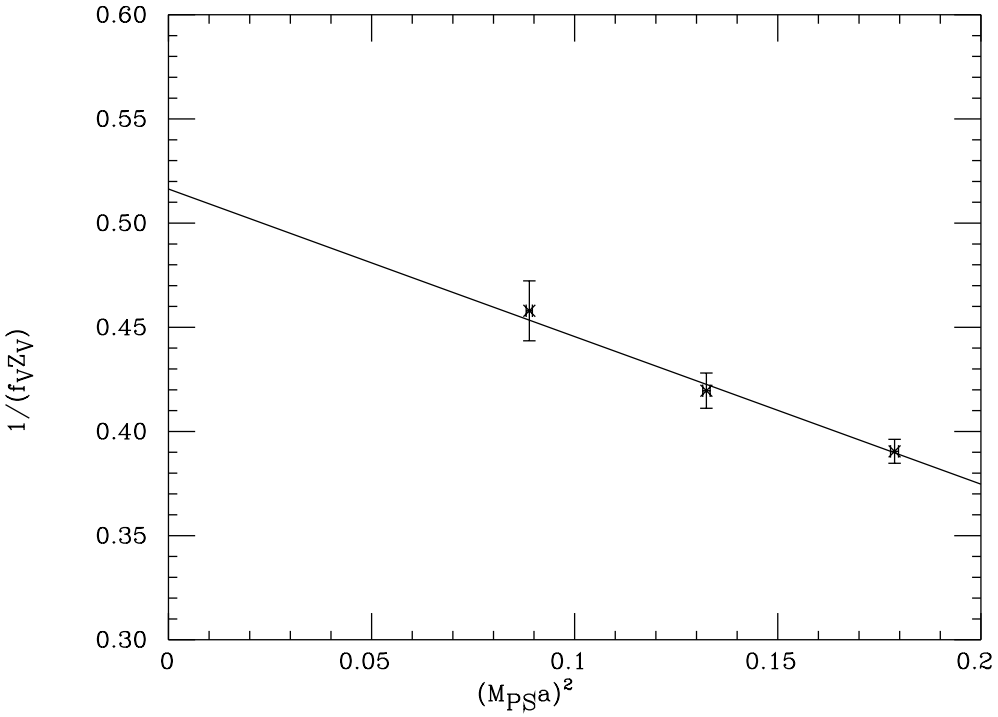

Fig. 9. As in fig. 6 for $\frac{1}{f_V Z_V}$.

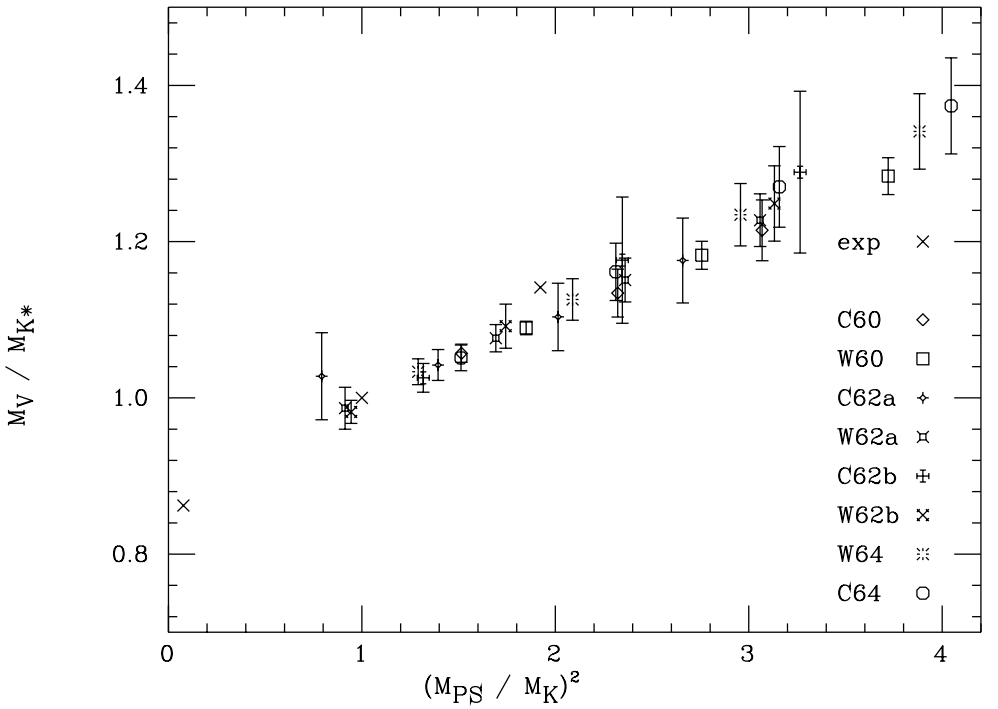

Fig. 10. Mass of vector meson M_V versus the squared pseudoscalar mass M_{PS}^2 for all lattices. M_V and M_{PS} normalized to the lattice value of M_{K^*} and M_K respectively.

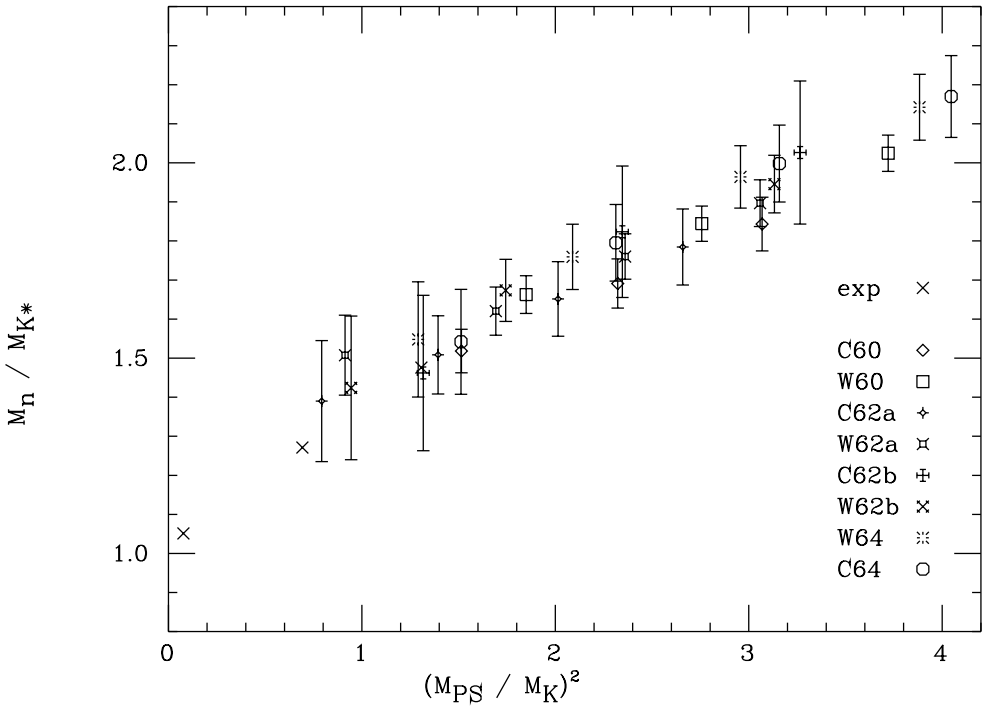

Fig. 11. As in fig. 10 for M_n.

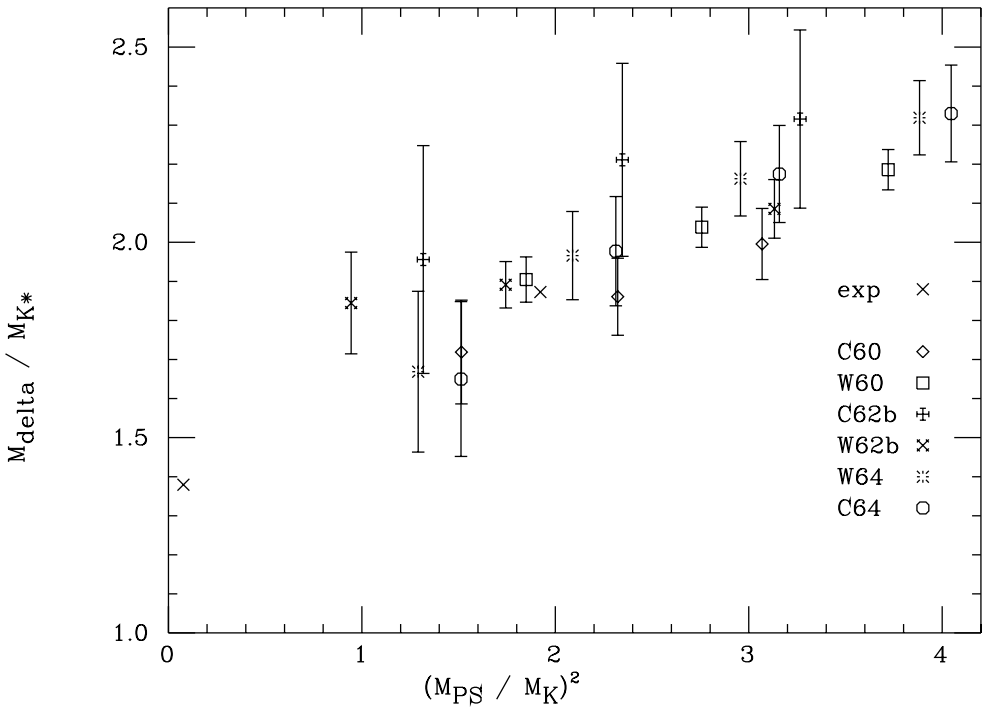

Fig. 12. As in fig. 10 for M_δ.

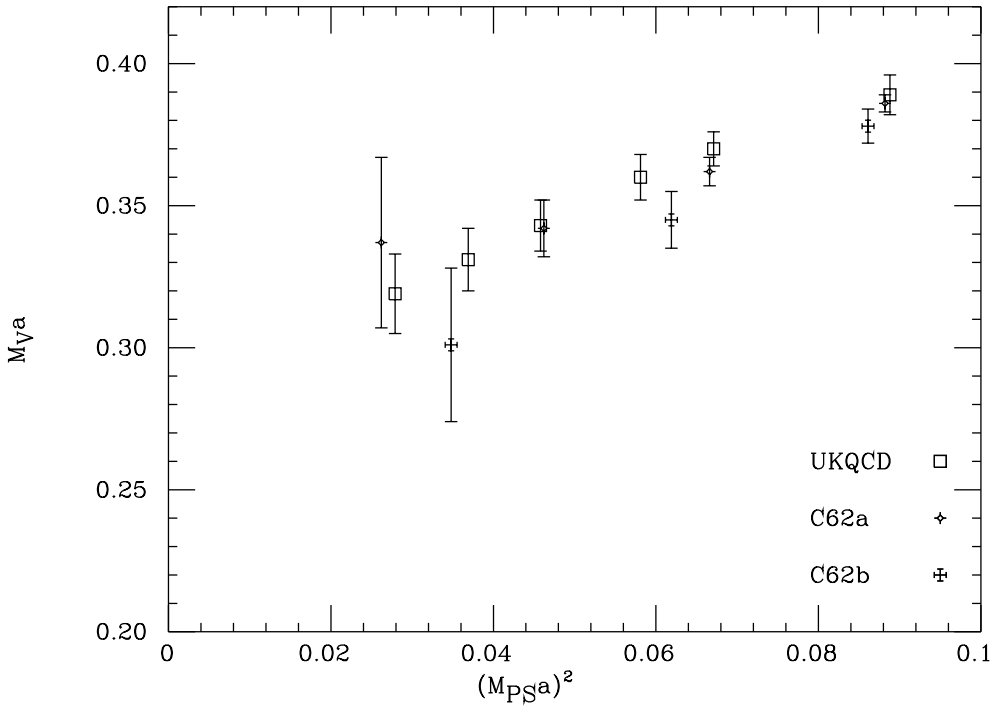

Fig. 13. Vector meson masses in lattice units at $\beta = 6.2$ for SW-Clover action from UKQCD [16], Lattice C62a and Lattice C62b.

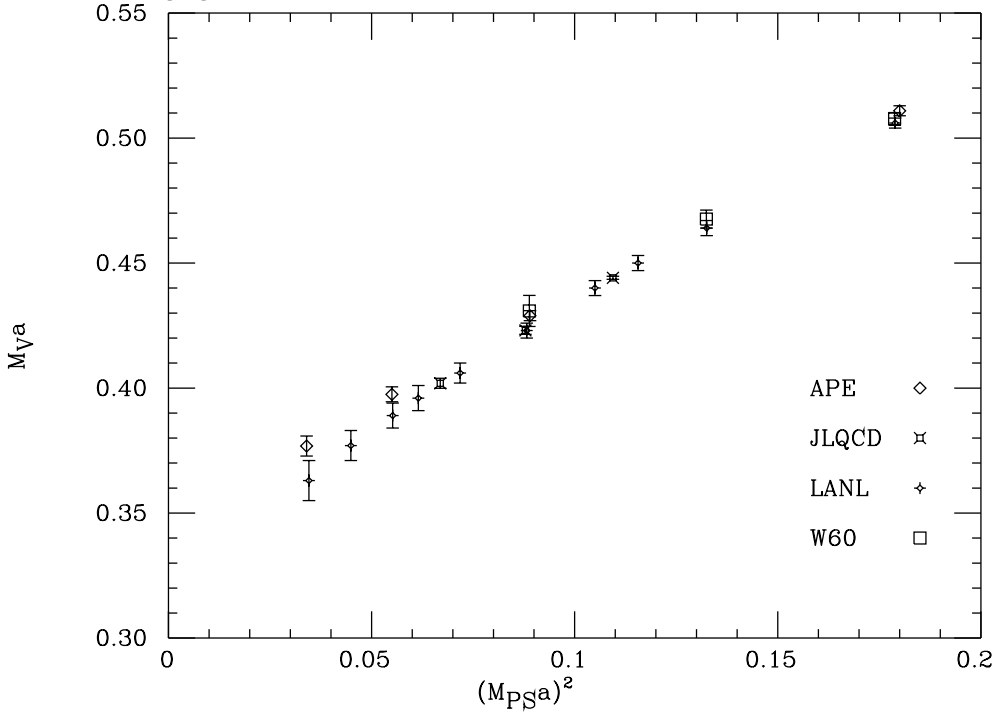

Fig. 14. Vector meson masses in lattice units at $\beta = 6.0$ for Wilson action from Lattice W60, APE $24^3 \times 32$ [25], JLQCD [11] and LANL [18].

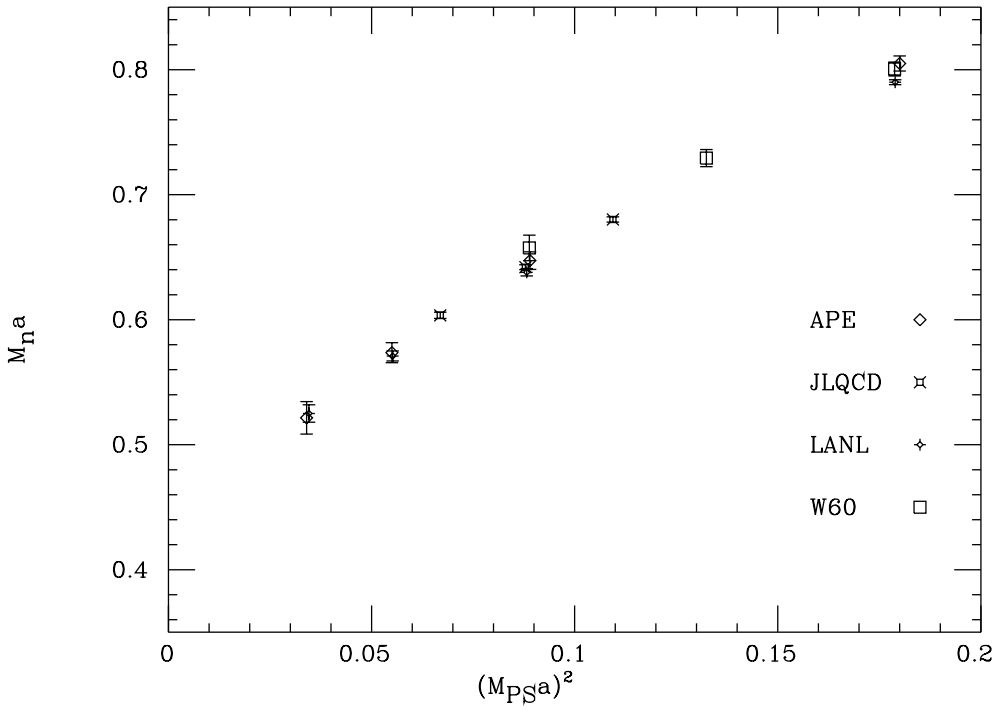

Fig. 15. Nucleon masses in lattice units at $\beta = 6.0$ for wilson action from Lattice W60, APE $24^3 \times 32$ [25], JLQCD [11] and LANL [18].

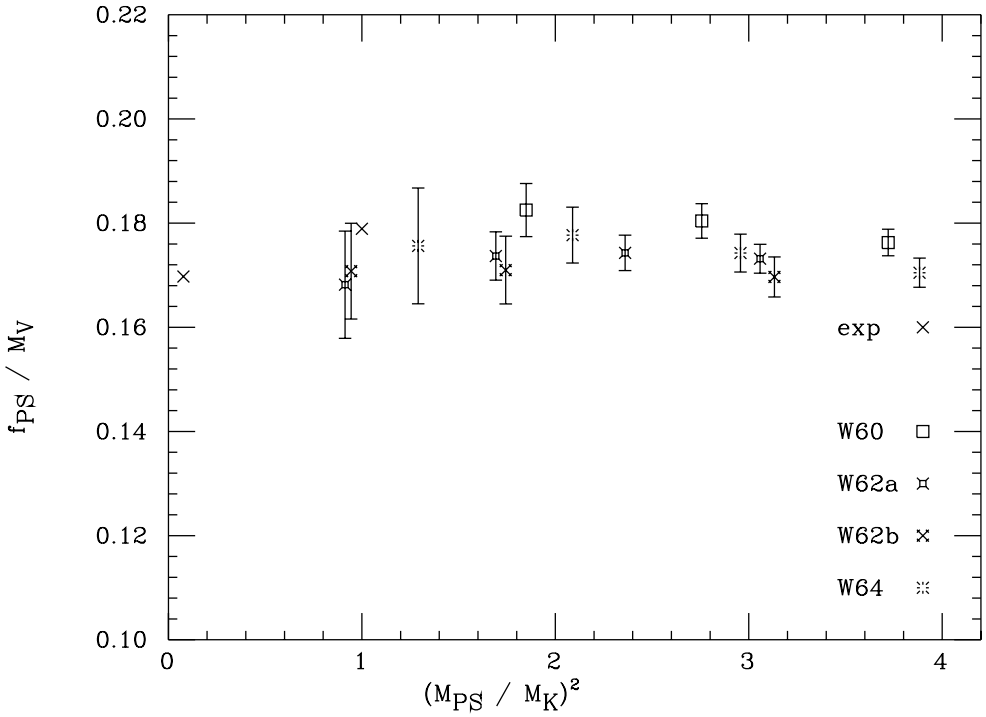

Fig. 16. Values of the ratio $\frac{f_{PS}}{M_V}$ versus the squared pseudoscalar mass M_{PS}^2 normalized to the lattice value of M_K for all lattices with Wilson action.

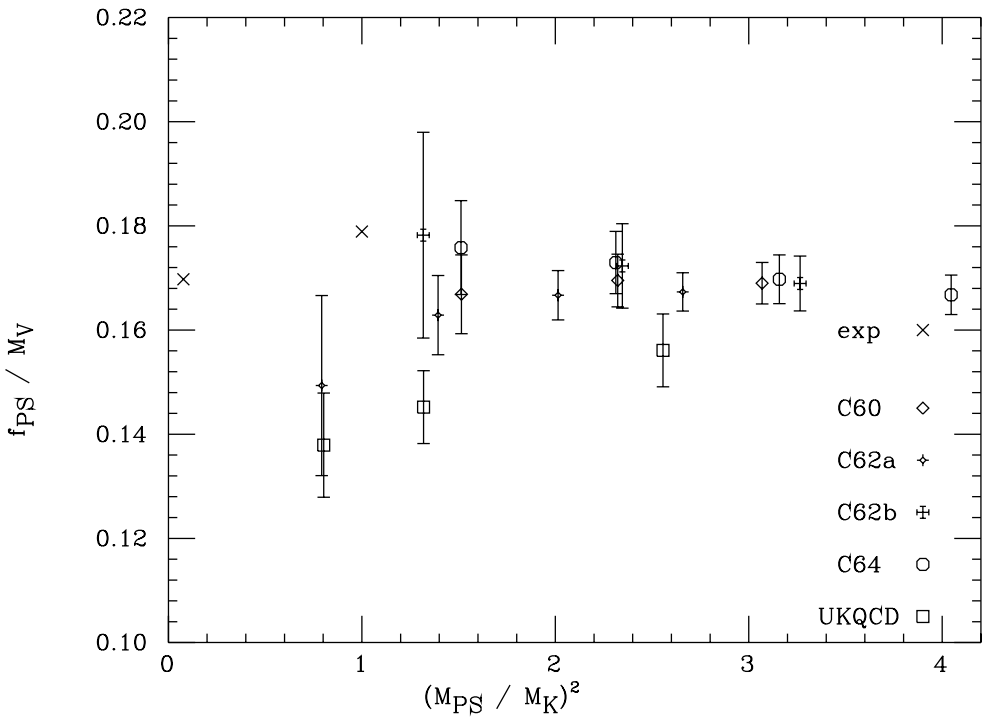

Fig. 17. Values of the ratio $\frac{f_{PS}}{M_V}$ versus the squared pseudoscalar mass M_{PS}^2 normalized to the lattice value of M_K for all lattices with SW-Clover action.

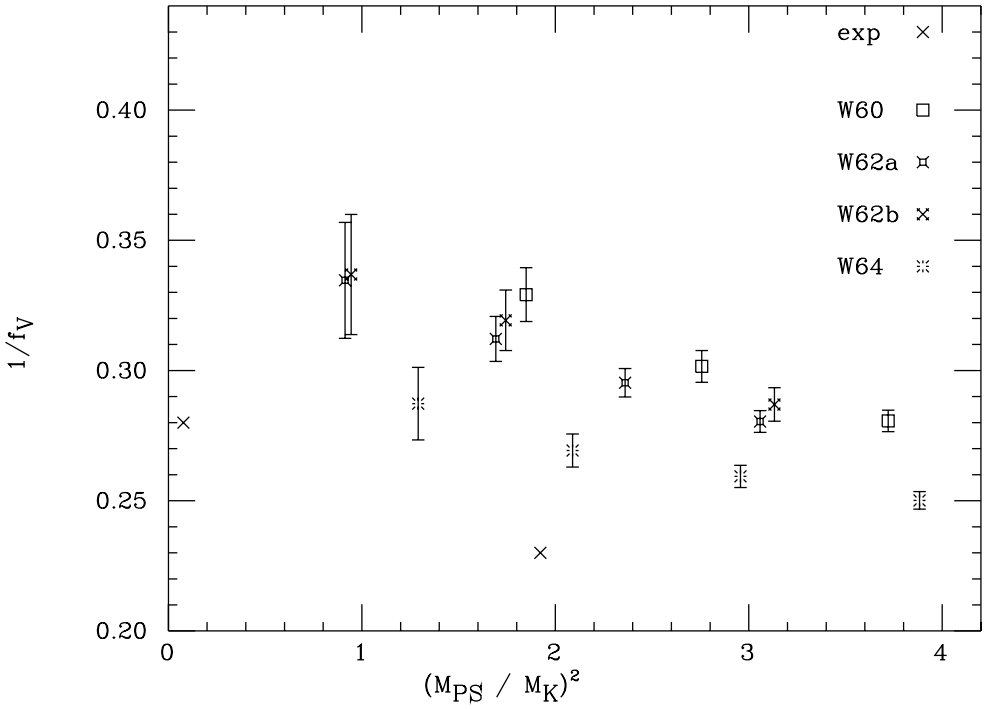

Fig. 18. Values of the vector decay constant $1/f_V$ versus the squared pseudoscalar mass M_{PS}^2 normalized to the lattice value of M_K for all lattices with Wilson action.

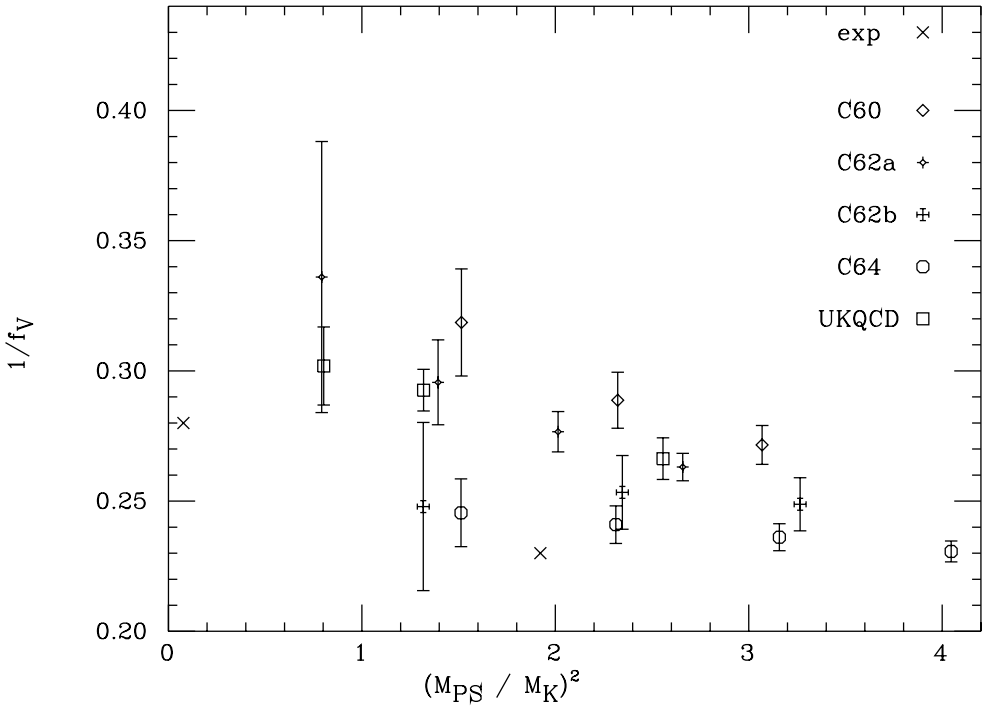

Fig. 19. Values of the vector decay constant $1/f_V$ versus the squared pseudoscalar mass M_{PS}^2 normalized to the lattice value of M_K for all lattices with SW-Clover action.

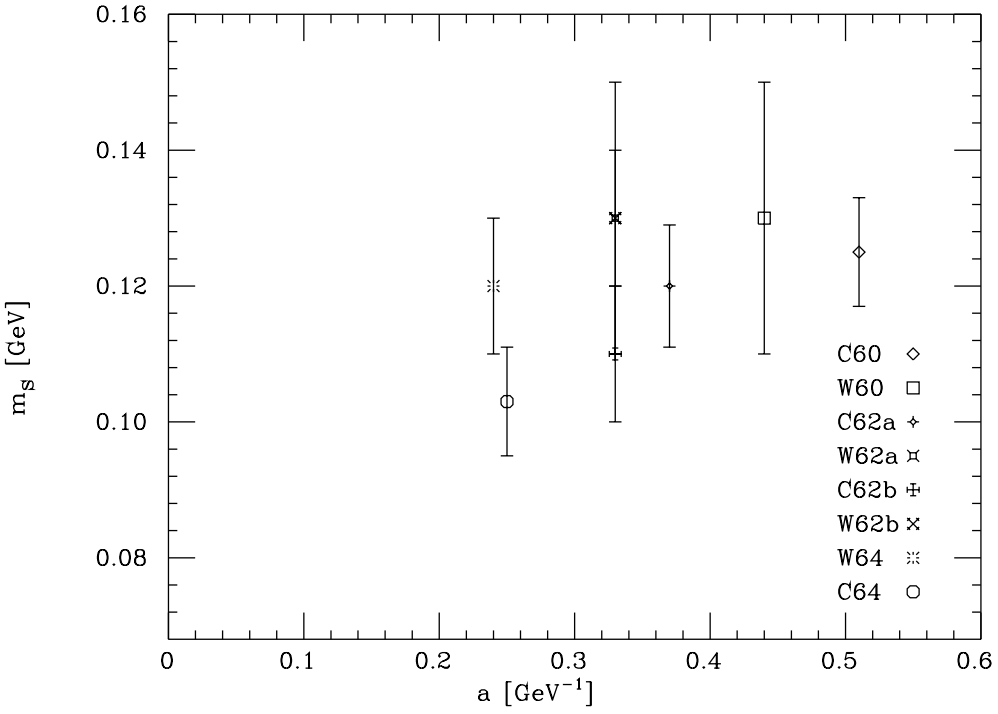

Fig. 20. Renormalized quark masses $m_s^{\overline{MS}}$ for all lattices.